International Journal of Mechanical, Industrial and Aerospace Sciences
ISSN: 2517-9950
Vol:7, No:3, 2013

Numerical Simulation and Experiment of a Lifting Body with Leading-Edge Rotating Cylinder

A. Badarudin, C. S. Oon, S. N. Kazi, N. Nik-Ghazali, Y. J. Lee, and W. T. Chong

***Abstract*—**An experimental and simulation flight test has been carried out to evaluate the longitudinal gliding characteristics of a lifting body with blunted half-cone geometry. The novelty here is the lifting body's pitch control mechanism, which consists of a pair of leading-edge rotating cylinders. Flight simulation uses aerodynamic data from computational fluid dynamics supported by wind-tunnel test. Flight test consists of releasing an aluminum lifting body model from a moving vehicle at the appropriate wind speed while measuring the lifting body's variation of altitude against time of flight. Results show that leading-edge rotating cylinder is able to give small amounts of improvement to the longitudinal stability and pitch control to the lifting body.

***Keywords*—**Lifting body, pitch control, aerodynamic, rotating cylinder.

I. Introduction

A lifting body is a wingless vehicle that flies due to the lift generated by the shape of its fuselage [1]. The lifting body program at National Aeronautics and Space Administration (NASA) started as an attempt to design an aircraft that could fly back from space in a smooth landing rather than a dangerous plunge to Earth in a ballistic entry. According to Monti et al. [2], high-risk and uncomfortable re-entry in a capsule will be unfeasible in the future as space transportation becomes more widespread; hence, safe, glider-like vehicles will become the choice for re-entry vehicle.

Lifting body is considered promising for such re-entry due to its favorable aerodynamic characteristics at high angle of attack. The lifting body studied here adopts the design of a blunt-nosed, half-cone vehicle without the main wing structure seen on most conventional aircraft which will cause excessive friction and heating. The flat part of the half-cone body surface can produce lift force while enhancing aerodynamic stability [3].

This study investigates the longitudinal gliding characteristics of a lifting body based on blunted half-cone geometry. The lifting body model used in this study has a novel feature in the form of a pair of leading-edge rotating cylinders. In terms of aircraft flight control systems, an aircraft is conventionally controlled by ailerons, elevators and rudders. Direct-lift control, which generates lift force directly without a change of aircraft incidence angle is also widely used; such as helicopters and VTOL (vertical take-off and landing) aircrafts [4]. More recent advancements include thrust vectoring and use of forebody strakes [5, 6]. There is also active research in hinge-less flight control such as using Piezo-fluidic actuators and plasma actuators [7, 8]. Hence, the novelty here is the application of rotating cylinders as a form of flight control, namely, to control the lifting body in pitch mode.

This study aims to evaluate the effectiveness of such leading-edge rotating cylinders in terms of pitch control by combining aerodynamic date, obtained from validated computational fluid dynamics (CFD) studies, with a flight simulator capable of calculating data such as airspeed, angle of attack, pitch angle, pitch rate and aircraft altitude. The flight characteristics of the lifting body with and without rotating cylinders are compared.

II. Methodology

Aerodynamic data of the lifting body with rotating cylinders was obtained by CFD and validated by wind-tunnel testing. For CFD, Unsteady calculation using PISO algorithm (Pressure Implicit with Splitting Operators) by Issa was used [9]. A steady state solver was not preferred as it was known to yield erroneous results for separated flow [10, 11], especially for aircraft with high angles of attack [12]. Turbulence model was handled by the unsteady Reynolds-averaged Navier Stokes (URANS) approach via Spalart-Allmaras turbulence model [13]. Second order total variation diminishing (TVD) discretisation scheme with Sweby's flux limiter was used for numerical stability [14]. Implicit time-stepping was used for temporal discretisation. The solution was obtained using the Open Source Field Operation and Manipulation C++ libraries (OpenFOAM). Grid independence study was carried out,

A. Badarudin is with Mechanical Department, Faculty of Engineering, University of Malaya, 50603 Kuala Lumpur, Malaysia (e-mail: ab01@um.edu.my).

C. S. Oon is with Mechanical Department, Faculty of Engineering, University of Malaya, 50603 Kuala Lumpur, Malaysia (corresponding author to provide phone: +60125036504; e-mail: oonsean2280@siswa.um.edu.my).

S. N. Kazi is with Mechanical Department, Faculty of Engineering, University of Malaya, 50603 Kuala Lumpur, Malaysia (e-mail: salimnewaz@um.edu.my).

N. Nik-Ghazali is with Mechanical Department, Faculty of Engineering, University of Malaya, 50603 Kuala Lumpur, Malaysia (e-mail: nik_nazri@um.edu.my).

Y. J. Lee is with Mechanical Department, Faculty of Engineering, University of Malaya, 50603 Kuala Lumpur, Malaysia (e-mail: leeyinjen@gmail.com).

W. T. Chong is with Mechanical Department, Faculty of Engineering, University of Malaya, 50603 Kuala Lumpur, Malaysia (e-mail: chong_wentong@um.edu.my).

showing insignificant variation of aerodynamic coefficients when number of grid cells was increased from 2.2 million to 5.1 million.

The lifting body's lift, drag and pitching moment coefficient, after the addition of leading-edge rotating cylinders as vortex control devices, are shown in Fig. 1, Fig. 2 and Fig. 3 respectively. Inwards cylinder rotation rate indicates the cylinder rotation direction where airflow is directed upwards and inwards towards the top surface of lifting body, in a direction parallel to mean flow; outwards cylinder rotation rate indicates the opposite direction. In Fig. 3, the lifting body showed a large tendency to pitch in a positive direction (nose-up), which could be circumvented partially by rotating the leading-edge cylinders in an inward direction.

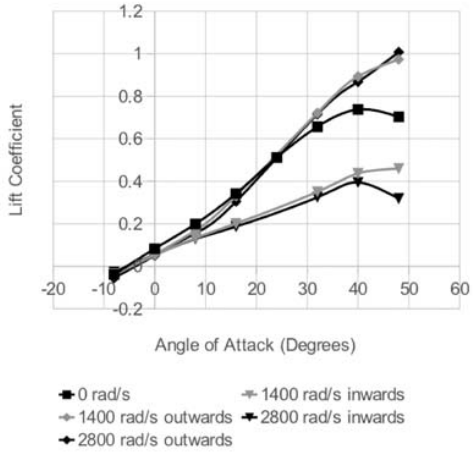

Fig. 1 Lift coefficient of lifting body at varying angles of attack and cylinder rotation

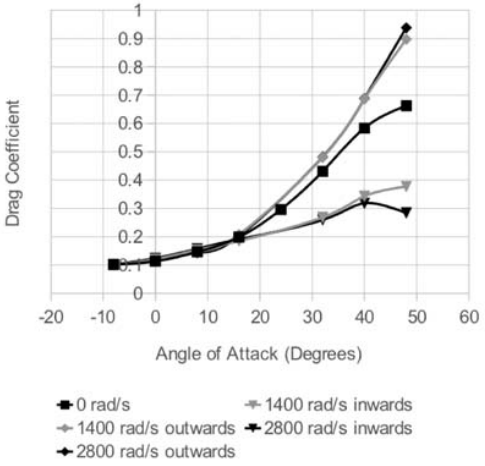

Fig. 2 Drag coefficient of lifting body at varying angles of attack and cylinder rotation

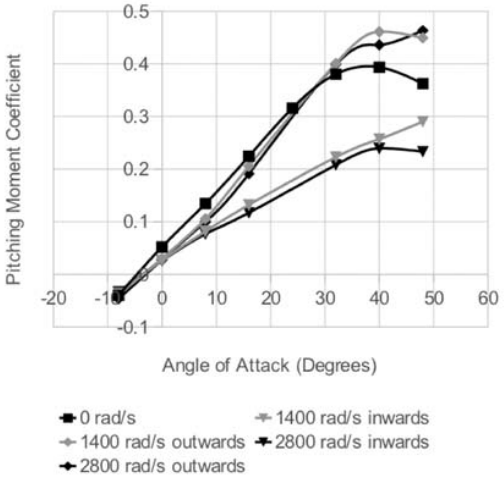

Fig. 3 Pitching moment coefficient of lifting body at varying angles of attack and cylinder rotation

The wind tunnel validation test was conducted using the low speed wind tunnel in the Aeronautics Laboratory Faculty of Mechanical Engineering, Universiti Teknologi Malaysia, Skudai, Malaysia. It is a low speed, closed-return type wind tunnel of 2.0m (width) × 1.5m (height) × 5.8m (length) test section. The test model had a frontal area of 0.0470m^2 at zero angle of attack, and with varying angles of attack, gave blockage ranging from 1.6% to 3.8% for the wind-tunnel experiments carried out. The reported flow quality of wind was: velocity uniformity error below 0.15º, temperature uniformity error below 0.2ºC, flow angle uniformity error below 0.15% and turbulence below 0.06%. Fig. 4 shows the comparison between computational and experimental results for lift, drag and pitching moment coefficient for the case without rotating cylinders. Reasonable agreement was obtained. Corrections to aerodynamic data were carried out to take into account the blockage effect.

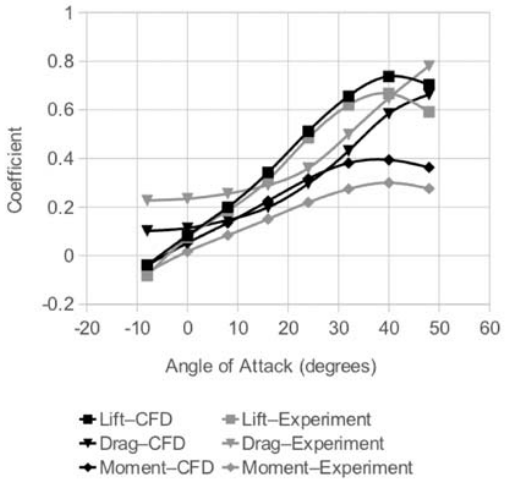

Fig. 4 Validation of lift, drag and pitching moment coefficient

III. Flight Simulation

Flight simulations were carried out to simulate longitudinal flight characteristics at subsonic speeds. The tool used to simulate the flight of lifting body was the F-16 fighter aircraft simulation tool by Klein and Morelli [15]. It was used to perform a nonlinear simulation on the lifting body developed and study the motion of that lifting body under different control inputs. The assumptions of the simulator include: (i) the rigid body of aircraft having constant mass density and symmetry about O_{XZ} plane in body axis, (ii) stationary atmosphere with altitudes below 15,000m, (iii) subsonic aircraft speeds, and (iv) uniform gravity field at 9.81m/s^2.

Full nonlinear, six-degree-of-freedom rigid-body translational and rotational aircraft motion was modeled, described by Newton's second law of motion. For translational motion, the governing equations are:

$$\dot{u} = rv - qw - g\sin\theta + \frac{\bar{q}SC_X + T}{m} \quad (1)$$

$$\dot{v} = pw - ru - g\cos\theta\sin + \frac{\bar{q}SC_Y}{m} \quad (2)$$

$$\dot{w} = qu - pv - g\cos\theta\cos + \frac{\bar{q}SC_Z}{m} \quad (3)$$

where u, v, w are translational velocity of aircraft in X-, Y- and Z-axis, respectively; p, q, r are the angular velocity of aircraft in X-, Y- and Z-axis, respectively; g is the acceleration due to gravity; Φ, θ and ψ are the roll, pitch and yaw angles, respectively; q is the dynamic pressure, S is the wing reference area, C_X, C_Y, C_Z are the body axis aerodynamic force coefficient in X-, Y- and Z-axis, respectively; T is the engine thrust force, m is the mass of aircraft.

For rotational motion, Newton's second law of motion gives:

$$\dot{p}I_x - \dot{r}I_{xz} = \bar{q}SbC_l - qr\left(l_z - l_y\right) + qpI_{xz} \quad (4)$$

$$\dot{q}I_y = \bar{q}S\bar{c}C_m - pr\left(I_x - I_z\right) - \left(p^2 - r^2\right)I_{xz} + rh_{eng} \quad (5)$$

$$\dot{r}I_z - \dot{p}I_{xz} = \bar{q}SbC_n - pq\left(I_y - I_x\right) - qrl_{xz} - qh_{eng} \quad (6)$$

where b is the wing span; S is the wing reference area; I is the moment of inertia of aircraft about certain axis; h_{eng} is the angular momentum vector for rotating mass of engine; C_l, C_m, and C_n are body axis aerodynamic rolling, pitching, yawing moment coefficient, respectively; p, q, r are the angular velocity of aircraft in X-, Y- and Z-axis, respectively.

The equations of motion above require some empirical properties to be defined. They include engine thrust force, aerodynamic force and moment coefficients, properties of air and mass properties of the vehicle. Each non-dimensional aerodynamic force and moment coefficient is built up from a set of component functions, which is in turn determined by a table look-up in the database with entries obtained from CFD. The value for each component function is found by linear interpolation, using current values of the states and controls. For values outside the range of available data, linear extrapolation is used.

In this study, finite differences were employed to linearise the nonlinear equations of motion. To obtain the state and output time series, the fourth-order Runge-Kutta scheme was utilized to perform numerical integration of the nonlinear equation of motion.

IV. Flight Testing

For the flight test, a lifting body prototype was built using aluminum sheets for the outer surface and aluminum bars for the support structure. The test model did not include the rotating leading-edge cylinders feature. A compartment was constructed to hold the Global Positioning System (GPS) unit, which was used to record flight data, as shown in Fig. 5. Data was recorded was the altitude of the model as it glided towards the ground. The GPS was mounted at the center of gravity of the prototype for accurate measurement of the lifting body model's position. The GPS unit used was GPSMAP 196 by Garmin, a versatile navigation device suitable for air, land and water types of transportation. The model was tested at the speed of 58.9km/h by launching the model from the window of a moving vehicle, after which it glided horizontally to the ground. Fig. 6 shows the comparison in terms of altitude between flight test and flight simulation. While the altitude at the start of the gliding flight was relatively well-predicted, significant deviation exists at the end of the data collection period.

Fig. 5 Lifting body flight test model with GPS unit

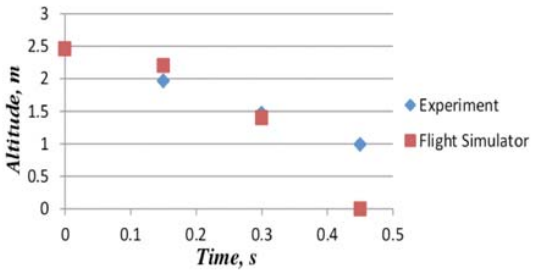

Fig. 6 Graph of altitude against time for both experimental and CFD simulation

Potential sources of error included ambient wind, as the experiment was done outdoors, and turbulent wake from the moving vehicle from which the model was released. Additionally, the geometry fabricated with aluminum did not follow the wind-tunnel test model exactly. There were some unavoidable deviations during fabrication as the aluminum sheets are bent by hand.

The data recorded was the altitude of the model as it glided towards the ground. Based on the comparison, it is assumed that the flight simulation to have acceptable accuracy compared to experiment. The effect of leading-edge rotating cylinders was then evaluated. For the flight simulation, the range of angle of attack was limited to a maximum of 50º. In other words, if the angle of attack reported by the flight simulator exceeded 50º, the flight was assumed to have stalled irrecoverably. Fig. 7 represents a normal horizontal gliding flight while Fig. 8 is the flight simulation under similar conditions, but with the leading-edge rotating cylinders spinning inwards at two times the free stream velocity in an attempt to control pitch and improve lifting body stability. Comparing the two diagrams, cylinder rotation slightly extended the time taken for the lifting body to reach the irrecoverable, 50 º angle of attack ranges, although its effects were not very significant. Nevertheless, the rotating cylinders were shown to have some contributions to increasing stability.

V. Conclusion

The effectiveness of a pair of leading-edge rotating cylinders in terms of pitch control has been evaluated by using aerodynamic data, obtained from CFD and validated with experimental wind-tunnel data. The flight characteristics were further validated using flight test data. CFD and wind tunnel data showed reasonable agreement while flight simulation and flight test data showed some deviations, partly due to the errors arising from the experiment. Results showed that a leading-edge rotating cylinder has contributed to improve the longitudinal stability of the lifting body.

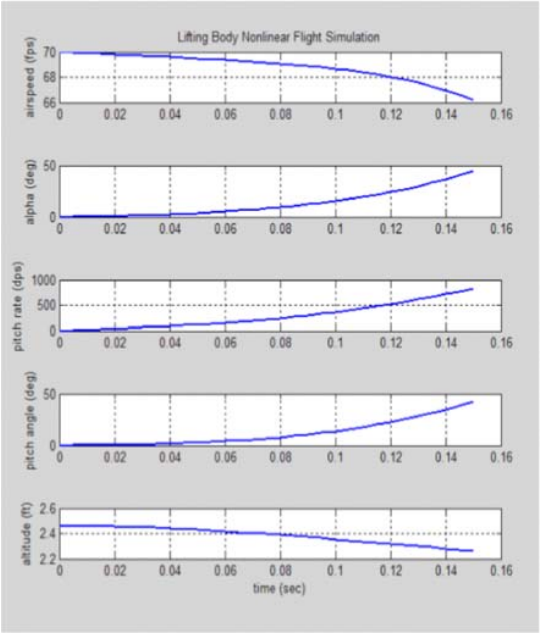

Fig. 7 Lifting body flight simulation results without leading-edge cylinder rotation

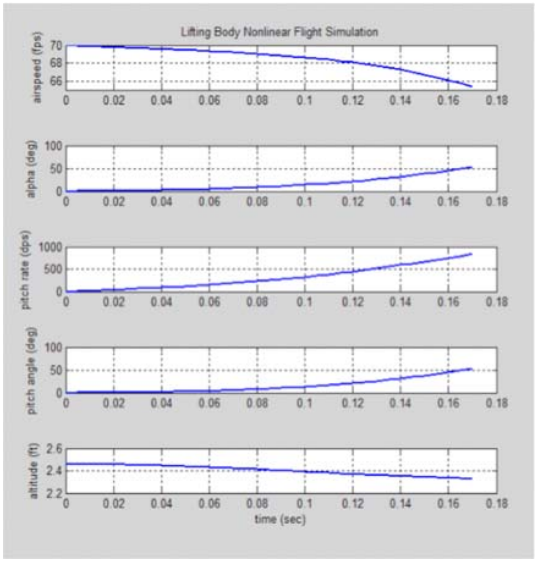

Fig. 8 Lifting body flight simulation with inwards leading-edge cylinder rotation

Acknowledgment

The authors gratefully acknowledge High Impact Research Grant UM.C/625/1/HIR/MOHE/ENG/46 and the Fundamental Research Grant Scheme, FP062/2010A, University of Malaya, Malaysia for support to conduct this research work.

References

[1] R.D. Reed, Wingless Flight: The Lifting Body Story, National Aeronautics and Space Administration, Washington, 1997.

[2] [2] R. Monti, D.M. Paterna, A low risk reentry: looking backward to step forward, Aerospace Science and Technology 10 (2006) 156–167.
[3] Y. Li, Y. Jiang and C. Huang, Shape design of lifting body based on genetic algorithm, International Journal of Information Engineering and Electronic Business 2 (2010) 37-43.
[4] W.J.G. Pinsker, The Control Characteristics of Aircraft Employing Direct-Lift Control, Aeronautical Research Council, London, 1970.
[5] C.W. Alcorn, M.A. Croom, M.S. Francis and H. Ross, The X-31 Aircraft: Advanced in Aircraft Agility and Performance, Progress in Aerospace Sciences 32 (1996) 377 – 413.
[6] F.J. Lallman, J.B. Davidson and P.C. Murphy, A Method for Integrating Thrust-Vectoring and Actuated Forebody Strakes with Conventional Aerodynamic Controls on a High-Performance Fighter Airplane, National Aeronautics and Space Administration, Hampton, 1998.
[7] A. Seifert, S. David, I. Fono, O. Stalnov, I. Dayan, S. Bauminger, R. Guedj, S. Chester and A. Abershitz, Roll Control via Active Flow Control: From Concept Development to Flight, Technion Israel Institute of Technology, 49th Israel Annual Conference on Aerospace Sciences, Tel Aviv, Israel, 2009.
[8] M.P. Patel, T.T. Ng, Srikanth Vasudevan, T.C. Corke and C. He, Plasma Actuators for Hingeless Aerodynamic Control of an Unmanned Air Vehicle, Journal of Aircraft 44 (2007) 1264–1274.
[9] H.K. Versteeg and W. Malalasekera, An introduction to Computational Fluid Dynamics: The Finite Volume Method, 2nd ed., Pearson Education Limited, Essex, 2007.
[10] G. Iaccarino, A. Ooi, P.A. Durbin and M. Behnia, Reynolds Averaged Simulation of Unsteady Separated Flow, International Journal of Heat and Fluid Flow 24 (2003) 147–156.
[11] P.R. Spalart, Strategies for Turbulence Modelling and Simulations, International Journal of Heat and Fluid Flow 21 (2000) 252–263.
[12] A. Schutte, O.J. Boelens, M. Oehlke, A. Jirasek, T. Loeser, Prediction of flow around the X-31 aircraft using three different CFD methods, Aerospace Science and Technology 20 (2012) 21–37.
[13] P.R. Spalart and S.R. Allmaras, A One Equation Turbulence Model for Aerodynamic Flows, AIAA (American Institute of Aeronautics and Astronautics), AIAA 30th Aerospace Sciences Meeting and Exhibit, Reno, United States of America, 1992.
[14] P.K. Sweby, High Resolution Schemes Using Flux Limiters for Hyperbolic Conservation Laws, SIAM Journal on Numerical Analysis 21 (1984) 995–1011.
[15] V. Klein and E.A. Morelli, Aircraft System Identification: Theory and Practice, American Institute of Aeronautics and Astronautics, Inc, Virginia, 2006.